Identification of motifs in cholera toxin A1 polypeptide that are required for its interaction with human ADP-ribosylation factor 6 in a bacterial two-hybrid system

Michael G. Jobling and Randall K. Holmes*

Department of Microbiology, University of Colorado Health Sciences Center, Denver, CO 80220

Edited by John J. Mekalanos, Harvard Medical School, Boston, MA, and approved October 20, 2000 (received for review September 14, 2000)

The latent ADP-ribosyltransferase activity of cholera toxin (CT) that is activated after proteolytic nicking and reduction is associated with the CT A1 subunit (CTA1) polypeptide. This activity is stimulated *in vitro* by interaction with eukaryotic proteins termed ADP-ribosylation factors (ARFs). We analyzed this interaction in a modified bacterial two-hybrid system in which the T18 and T25 fragments of the catalytic domain of *Bordetella pertussis* adenylate cyclase were fused to CTA1 and human ARF6 polypeptides, respectively. Direct interaction between the CTA1 and ARF6 domains in these hybrid proteins reconstituted the adenylate cyclase activity and permitted cAMP-dependent signal transduction in an *Escherichia coli* reporter system. We constructed improved vectors and reporter strains for this system, and we isolated variants of CTA1 that showed greatly decreased ability to interact with ARF6. Amino acid substitutions in these CTA1 variants were widely separated in the primary sequence but were contiguous in the three-dimensional structure of CT. These residues, which begin to define the ARF interaction motif of CTA1, are partially buried in the crystal structure of CT holotoxin, suggesting that a change in the conformation of CTA1 enables it to bind to ARF. Variant CTA polypeptides containing these substitutions assembled into holotoxin as well as wild-type CTA, but the variant holotoxins showed greatly reduced enterotoxicity. These findings suggest functional interaction between CTA1 and ARF is required for maximal toxicity of CT *in vivo*.

Cholera, caused by the Gram-negative intestinal pathogen *Vibrio cholerae*, remains a significant cause of morbidity and mortality in the developing world. Cholera toxin (CT), the primary virulence factor produced by the bacterium, is responsible for the massive dehydrating diarrhea characteristic of the disease (1). CT is secreted by the bacterium into the external milieu as an oligomeric complex of a single enzymatic A subunit (CTA) noncovalently coupled to a pentamer (CTB) of identical B subunits, and it has latent ADP-ribosyltransferase activity. The A subunit has a single intramolecular disulfide bond between Cys-187 and Cys-199, forming a protease-sensitive loop (2). Nicking within this loop by bacterial or host proteases generates the CTA1 and CTA2 polypeptides. CTA1 contains the enzyme active site, and CTA2 tethers the A1 polypeptide to CTB. Both nicking and reduction of the disulfide bond are required for full enzymatic activity (3). CTB binds to its receptor, ganglioside GM_1, on the surface of enterocytes. After internalization of CT and reduction of CTA, CTA1 gains access to the cell cytosol and catalyzes the NAD-dependent ADP ribosylation of the α subunit of the regulatory heterotrimeric G protein, Gs, inhibiting its GTPase activity and locking it in an active form. The consequence is constitutive stimulation of adenylate cyclase activity and increased intracellular cAMP levels (4), leading to fluid and electrolyte secretion by the affected enterocytes and the massive diarrhea characteristic of cholera.

The enzymatic activity of CTA1 (and related *Escherichia coli* heat-labile enterotoxins) is greatly stimulated by host-cell proteins called ADP-ribosylation factors (ARFs; refs. 5 and 6). ARFs are members of a highly conserved multigene family of small GTP-binding proteins, originally identified as activators of CT. They interact with several other proteins and are ubiquitously involved in membrane trafficking events (7). ARFs must be in the GTP-bound form to be active. There are six mammalian ARFs (five human) that fall into three classes: ARFs 1, 2, and 3 (class I), ARFs 4 and 5 (class II), and ARF6 (class III). Class I ARFs regulate the assembly of several types of vesicle coat complexes (8). Little is known of the function of class II ARFs. ARF6 is found at the cell periphery and regulates vesicle movement between endosomes and the plasma membrane (9–11). All ARFs can be myristylated at the conserved N-terminal glycine, which promotes membrane association of the GTP-bound forms (12).

Although CT–ARF interaction has been characterized biochemically in great detail (13), little is known about their physical interaction. ARFs do not interact with native CT, and nicking and reduction are prerequisites for exposure of an ARF-binding site on CTA1 (14). Determining how CTA1 and ARF interact should help explain why CTA1 requires ARF for optimal enzymatic activity, and it could provide new insights about trafficking of CT from the plasma membrane to the cytosol. In this study, we modified a recently described bacterial two-hybrid system that is based on the reconstitution of a signal-transduction pathway (15), and we used it to show that recombinant CTA1 and human ARF6 polypeptides can interact directly in the bacterial cytoplasm. We selected variants of CTA1 that do not interact with ARF6 in this system, and we showed that the amino acid substitutions responsible for the observed phenotype were widely separated in the primary amino acid sequence of CTA1 but contiguous in the three-dimensional structure of CT. These findings begin to define the motif of CTA1 that constitutes its interaction interface with ARF. In intact CTA, these substitutions did not affect the structure of holotoxin but dramatically decreased its enterotoxicity, suggesting interaction of CTA1 with ARF is required for maximal toxicity of CT *in vivo*.

Materials and Methods

Bacterial Strains and Growth Media. *E. coli* TE1 is a Δ*endA* derivative of TX1 [F′::Tn*10 proA*$^+$*B*$^+$ *lacI*^{q} Δ(*lacZ*)*M15*, *glnV44*

This paper was submitted directly (Track II) to the PNAS office.

Abbreviations: CT, cholera toxin; CTA1, CT A1 subunit; CTA2, CT A2 subunit; ARF, ADP-ribosylation factor; wt, wild type; IPTG, isopropyl-β-D-thiogalactoside.

*To whom reprint requests should be addressed at: University of Colorado Health Sciences Center, Department of Microbiology, B175, 4200 E. 9th Avenue, Denver, CO 80220. E-mail: Randall.Holmes@UCHSC.edu.

The publication costs of this article were defrayed in part by page charge payment. This article must therefore be hereby marked "*advertisement*" in accordance with 18 U.S.C. §1734 solely to indicate this fact.

Article published online before print: *Proc. Natl. Acad. Sci. USA*, 10.1073/pnas.011442598. Article and publication date are at www.pnas.org/cgi/doi/10.1073/pnas.011442598

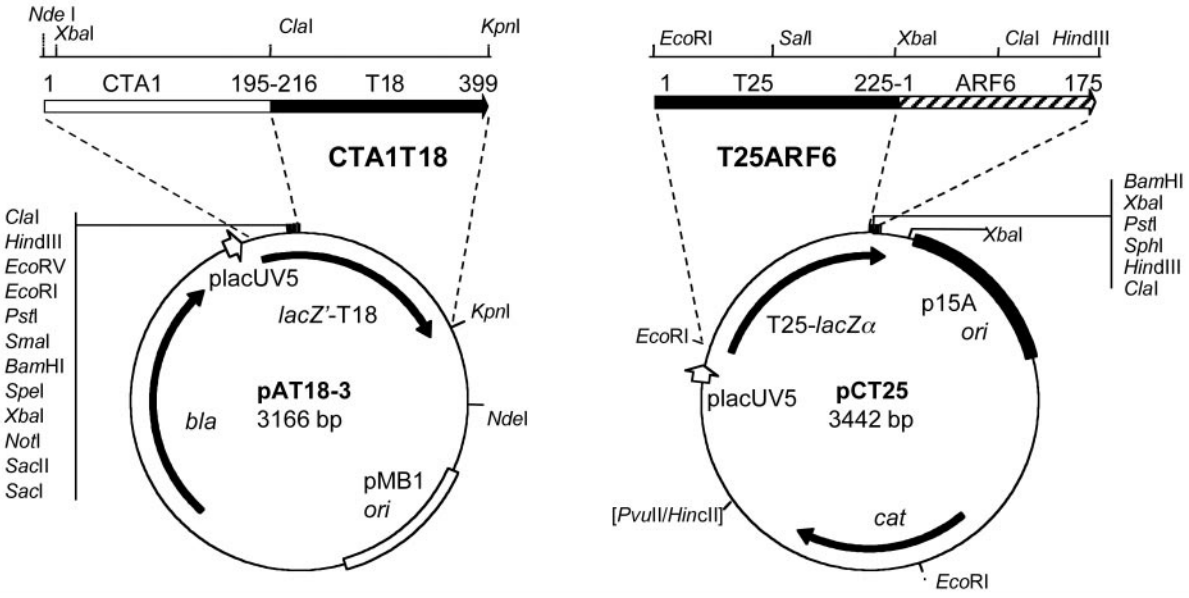

Fig. 1. Schematic representations of vectors and two-hybrid fusion constructs. Vectors are shown as circles within which filled arrows represent the β-lactamase (*bla*) and chloramphenicol acetyl transferase (*cat*) genes, and the lacZ-T18 and T25-lacZα ORFs. Open and solid boxes represent the pMB1 and p15A origins of replication, respectively. The *lacUV5* promoters are shown as open arrowheads that indicate the direction of transcription. Restriction maps for the DNA fragments encoding the CTA1T18 and T25ARF6 hybrid proteins are shown above the vectors. Dashed lines show fragments inserted into vectors to make the clones: CTA1 ORF (open box) linked to the T18 ORF (solid arrow) in pCTA1T18 and derivatives; T25 ORF (solid box) linked to ARF6 ORF (hatched arrow) in pT25ARF6. Numbers above ORFs correspond to the residues of the native proteins included in the fusion polypeptides.

Δ*(hsdM-mcrB)5* Δ (*lac-proAB) thi*] (16). TE1DC is a Δ*cyaA*::Km derivative of TE1 constructed by P1 transduction of kanamycin (Km^R) from SP850 (17). DH1D is a stable adenylate cyclase-deficient derivative (Δ*cyaA*::Km) of DH1 (F^-, *glnV44*, *recA1*, *endA1*, *gyrA96*, *thi1*, *hsdR17*, *spoT1*, *rfbD1*) (18) also constructed by P1 transduction from SP850. To enable P1 transduction, DH1 was made transiently $recA^+$ as described (19). Cultures were grown in LB at 30 or 37°C. Sugar fermentation was monitored by growth on MacConkey agar plates supplemented with 1% maltose. Antibiotics were added at 50 μg/ml (each, ampicillin and methicillin together, Ap^R) or 25 μg/ml for chloramphenicol (Cm^R) or Km^R.

Vector Construction. The bacterial two-hybrid system of Karimova *et al.* (15) was reconstructed in a modified form with different polylinker cloning sites flanking the T18 and T25 domains in their respective vectors to permit facile cloning of the CTA1 and ARF coding sequences. Briefly, coding regions for the T25 and T18 domains of adenylate cyclase were amplified by PCR from chromosomal DNA from a clinical isolate of *Bordetella pertussis* by using primers that incorporated unique restriction sites. Forward and reverse primers for the T18 domain (residues 214–399) were GCGGCGA**ATCGAT**GACCGATTTACCT (*Cla*I) and GCC**GGTGGTACCAT**GCGTTCCACTGCGCCCA (*Kpn*I, and an ochre stop codon), respectively, and for the T25 domain (residues 1–225) they were GACA**GAATCC**CATG-CAGCAATCGCATCAG (*Eco*RI) and G**GGATCC**CGC-CGCGTGCGCGCC (*Bam*HI), respectively. Bold bases that differ from the *cya* gene sequence were changed to introduce the underlined restriction sites (shown in parentheses) or stop codon. The T25 domain was cloned as an *Eco*RI-*Bam*HI fragment into pK187 to make pKT25 (Km^R). The vector pCT25 (Fig. 1) was made by cloning a *Pvu*II-*Hin*dIII fragment of pKT25 carrying the *lacUV5* promoter and T25-encoding region into *Hin*cII-*Hin*dIII cut pACYC184 (20). The T18 domain was cloned as a *Cla*I-*Kpn*I fragment into pBluescript SKII+ (Stratagene) to make pAT18. The vector pAT18–3 (Fig. 1) was made in several steps, resulting in subcloning of the *lacUV5* promoter and T18 domain from pAT18 into the backbone of a lower copy number vector, pT7–5 [a derivative of pT7–1 (21)].

The clone pT25ARF6 was made by first PCR amplifying the human ARF6 gene from pT7arf6 (a gift from Joel Moss, National Institutes of Health) by using primers that incorporated *Xba*I and *Hin*dIII sites at the 5′ and 3′ ends of the gene, GAGA**TCTAGA**TATGGGGAAGGTGC and AACT**AAGCT-T**CCTTTCGGGC, respectively, followed by cloning of the *Xba*I-*Hin*dIII digested PCR product into pKT25, to make pKT25ARF6. A *Pvu*II-*Hin*dIII fragment from pKT25ARF6, carrying the *lacUV5* promoter and T25ARF6 gene fusion, was then cloned into *Hin*cII-*Hin*dIII cut pACYC184 to make pCT25ARF6 (Fig. 1).

The CTA1T18 derivatives were made by replacing the *lacZ* translation initiation and polylinker of the pAT18 vector with a gene encoding the mature CTA1 polypeptide (residues 1–195). This gene is expressed from the T7 gene 10 translation initiation signal and was joined at the natural *Cla*I site of CTA1 to the T18 domain to create pCTA1T18. In plasmid $pCTA1_{DD}T18$, the wild-type (wt) *Xba*I-*Cla*I fragment was replaced with a variant fragment encoding E110D and E112D substitutions in CTA1. Plasmids pCTA1T18–2 and $pCTA1_{DD}T18$–2 carry the CTA1T18 fusions of pCTA1T18 and $pCTA1_{DD}T18$, respectively, in the lower copy number vector pAT18–3. Finally, $pCTA1_{R7K}T18$–2 encodes an R7K variant of CTA1 cloned in pAT18–3 (Fig. 1).

Two-Hybrid Screening. Interaction between CTA1T18 and T25ARF6 fusion proteins leading to the cytoplasmic production and assembly of functional adenylate cyclase in *E. coli* strains was detected qualitatively by the ability to ferment maltose (and thus formation of red colonies with or without precipitation of the bile salts) on maltose–MacConkey agar plates. Quantitative data were obtained by measuring the cAMP-induced expression of β-galactosidase activity, expressed in Miller units (22), from triplicate cultures of DH1DC[pT25ARF6] transformed with

MICROBIOLOGY

vector, wt, or variant CTA1T18 derivatives, and grown overnight at 30°C in LB.

Generation and Characterization of Clones Expressing Variant CTA1T18 Gene Fusions. Two rounds of PCR amplification (30 cycles each) were done by using pARCT5 (a CT clone with a unique *Pst*I site within *ctxA1*) as template, with primers that flank the *Xba*I and *Cla*I sites in *ctxA*1, to amplify the majority of the A1 gene and to introduce random mutations because of the low fidelity of *Taq* DNA polymerase. PCR products were purified, digested with *Xba*I and *Cla*I, and the 552-bp fragment encoding CTA1 residues 10–195 was ligated back into $pCTA1_{R7K}T18$–2. The ligation products were transformed into TE1DC[pT25ARF6] with selection for Ap^R Cm^R on maltose–MacConkey plates at 30°C [with or without 12.5 μM isopropyl-β-D-thiogalactoside (IPTG)] to generate a library of potential variants of $CTA1_{R7K}T18$ fusion proteins with decreased ability to interact with T25ARF6. Putative variants picked directly from maltose–MacConkey plates were screened for production of the full-length $CTA1_{R7K}T18$ fusion protein by Western blotting, by using a rabbit anti-CTA antibody and chemiluminescent detection as described by the manufacturer (Renaissance Kit, DuPont/NEN). The DNA sequences (and deduced amino acid sequences) of selected variants were then determined, and the *Xba*I-*Cla*I fragment encoding each variant was transferred into pARCT4, a clone expressing CT holotoxin under the control of an arabinose promoter (23). Transfer of the mutation was confirmed by screening for the *Pst*I site present in *ctxA1* from the mutant allele and absent from pARCT4. CT expression was induced with 0.5% L-arabinose for 3 h at 30°C, and periplasmic extracts were made in Tris-buffered saline containing 1 mg/ml polymyxin B sulfate. Holotoxin and free B pentamer were quantitated by GM_1-ELISA (24) by using anti-CTA and anti-CTB specific primary antibodies and purified CT holotoxin as the standard, and toxicity was assayed in mouse Y1 adrenal cell bioassays (25). Sensitivity of variant holotoxins to limited treatment with trypsin was determined by treating them for 30 min with 2% (wt/vol) bovine trypsin at 30°C. The reactions were stopped with 4% (wt/vol) of soybean trypsin inhibitor. Proteolytic cleavage of the variant toxins was assessed by reducing SDS/PAGE and Western blotting with anti-CTA primary antibody. CTA in wt holotoxin is nicked by trypsin to generate CTA1 and CTA2, which are resistant to further proteolytic degradation.

Site-Directed Mutagenesis. Mutations encoding V97K and Y104K substitutions were introduced into $pCTA1_{R7K}T18$–2 by using the Quick-Change system as described (Stratagene) with the following oligonucleotides (along with their reverse complement oligonucleotides; base changes in bold): V97K CAACATGTTTAAC**AAA**AATGATGTATTAG (loses *Psp*1406I, AACGTT); Y104K (adds *Hha*I) GATGTATT**AG**GCGCAAAGAGTCCTCATCC. Restriction sites (underlined) were introduced or eliminated to facilitate screening, without additional changes to the encoded polypeptide.

Results

Construction of Plasmids Expressing CTA1T18 and T25ARF6 Hybrid Proteins. The bacterial two-hybrid system used in this study is based on the reconstitution of the cAMP signal transduction pathway in a *cyaA*-deficient strain of *E. coli*. This is caused by the fusion partner-directed association in the bacterial cytoplasm of two complementary fragments (T25 and T18) constituting the catalytic domain of *B. pertussis* adenylate cyclase (26). As described in *Materials and Methods*, we constructed vectors (pCT25 and pAT18) similar to the pT25 (pACYC184-derived, p15A replicon) and pT18 (pBluescript, pMB1 replicon) pair described previously (15), but with different multiple cloning sites. A DNA fragment gene encoding the full length enzymatically active mature CTA1 polypeptide (residues 1–195), minus its native signal sequence, was joined in frame to the 5′ end of the DNA encoding the T18 domain (residues 216–399) in pAT18. The resulting plasmid, pCTA1T18, encodes the 378-aa cytoplasmic fusion protein CTA1T18 (Fig. 1*A*), which is predicted to have an N-terminal Met preceding the Asn+1 of native mature CTA1. In plasmid pT25ARF6 (Fig. 1*B*), the coding region for the human ARF6 polypeptide was joined to the 3′ end of the coding region of the T25 domain to produce the 412-residue cytoplasmic T25ARF6 fusion protein, joining residues 1–225 of T25 via a short linker encoding DPLDM to residues 1–175 of ARF6. The seven-residue sequence MTMITNS derived from the vector polylinker *lacZ* sequence is predicted to precede the Met+1 residue of T25 in all constructs.

Production of Adenylate Cyclase by Functional Complementation Between CTA1T18 and T25ARF6 Proteins and Optimization of the System. The reporter strain DHP1 made by Karimova *et al.* (15) is a spontaneous *cya* mutant, and cya^+ revertants accumulate rapidly under storage conditions or during prolonged incubation on plates. Strain TE1DC, containing a stable deletion/insertion in *cyaA*, was constructed to avoid this problem of reversion. Although TE1DC carries $lacI^q$ on an F′ plasmid, the multicopy plasmids used for the two-hybrid analysis titrate enough LacI to prevent full repression. Furthermore, expression of the fusion proteins in both vectors is driven by the *lacUV5* promoter, which is independent of cAMP and the catabolite gene activator protein. Therefore, induction by IPTG was not required for detectable expression of the fusion proteins.

Strains TE1DC[pAT18, pCT25], TE1DC[pCTA1T18, pCT25], and TE1DC[pAT18, pT25ARF6] formed colorless colonies on maltose–MacConkey plates at 37°C (Fig. 2*A*, 3–5), showing they were unable to use maltose and there was no functional interaction between the T18 and T25 domains in these control strains. Only TE1DC[pCTA1T18, pT25ARF6] formed red colonies (Fig. 2*A*, 2), indicating the productive interaction between the T18 and T25 domains when they were present in the fusion proteins containing the CTA1 and ARF6 polypeptides, respectively. Although this interaction was clearly evident at 37°C, it was not seen at 30°C (Fig. 2 *A*–*C*, 2). Because the T18 fusions were expressed from a very high copy number plasmid (500–700 copies/cell), and the T25 fusions were expressed from a much lower copy number replicon (8–15 copies/cell), we constructed the vector pAT18–3 with a copy number similar to a *rom* mutant of pBR322 (20–30 copies/cell) to bring the gene dosage of the T18 fusion closer to that of the T25 fusion. TE1DC[pCTA1T18–2, pT25ARF6], expressing the CTA1T18 fusion from this lower copy number vector, showed functional interaction between CTA1 and ARF6 at both 30 and 37°C (Fig. 2 *B* and *C*, 7). Under the same conditions, TE1DC[pAT18–3, pT25ARF6] formed colorless or very pale pink colonies (Fig. 2 *B* and *C*, 6).

Colonies formed by strains containing either pCTA1T18 or pCTA1T18–2 with pT25ARF6 were noticeably smaller than those formed by strains containing the parental vector (pAT18 or pAT18–3, Fig. 2 *B* and *C*). These findings suggested that expression of the fusion proteins containing a wt CTA1 domain was toxic for *E. coli*, possibly as a consequence of ADP ribosylation of cellular proteins or hydrolysis of NAD. Furthermore, coexpression of a fusion protein containing ARF6 might exacerbate any potential toxic effects by increasing the activity of CTA1. Replacing the sequence encoding wt CTA1 with an allelic sequence encoding an enzymatically inactive variant (CTA1-E110D + E112D) in the low copy-number construct $pCTA1_{DD}T18$–2 greatly increased the ability of strains bearing the complementing plasmids to ferment maltose (forming dark red colonies on MacConkey agar plates)

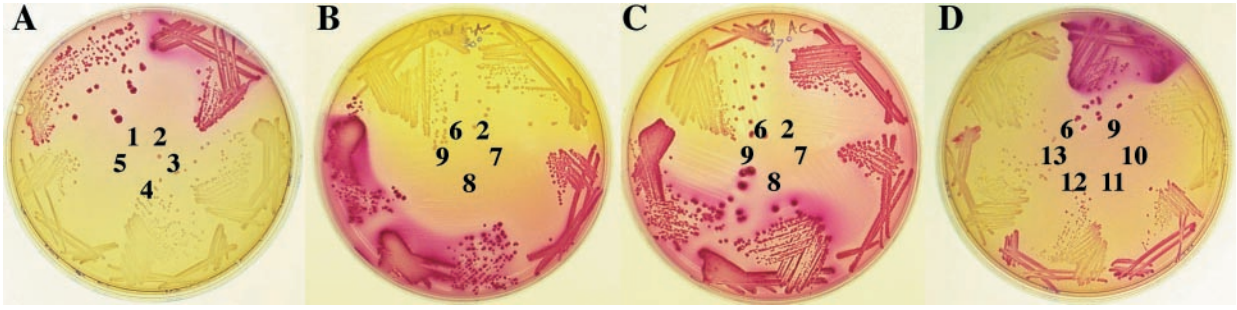

Fig. 2. Observed phenotypes in the two-hybrid system of vector controls, wt and variant fusion constructs on maltose–MacConkey plates in *E. coli* TE1DC. Growth conditions were 40 h at 37°C (*A*, initial constructs, and *C*, initial vs. optimized constructs) or 30°C (*B*, initial vs. optimized constructs) and 28 h at 30°C (*D*, representative variants). Numbers denote strains carrying the following plasmids (T18 derivatives in strains 1–5 are high copy number): (1) Positive control pT25zip + pT18zip (15); (2) pCTA1T18 + pT25ARF6; (3) pCTA1T18 + pCT25 vector; (4) pAT18 vector + pT25ARF6; (5) pAT18 + pCT25 vectors. Strains 6–13 all contain pT25ARF6 with the following low copy number T18 derivatives: (6) pAT18–3 vector; (7) pCTA1T18–2; (8) pCTA1$_{DD}$T18–2; (9) pCTA1$_{R7K}$T18–2. Strains 10–13 carry the following variants of pCTA1$_{R7K}$T18–2: (10) H171Y; (11) D99N; (12) N40D; (13) H44Y.

and to precipitate bile salts in the surrounding agar medium, dramatically shortening the time needed to observe the color change (Fig. 2 *B* and *C*, 8).

Isolation of CTA1 Variants Defective in ARF Interaction. To facilitate the analysis of potential variants of CTA1 that do not interact with ARF6, we constructed pCTA1$_{R7K}$T18–2, encoding the enzymatically inactive R7K variant of CTA1, encoded by a mutation located external to the *Xba*I-*Cla*I fragment that encodes residues 10–195 of CTA1. TE1DC[pCTA1$_{R7K}$T18–2, pT25ARF6] had a maltose-utilization phenotype identical to TE1DC[pCTA1$_{DD}$T18, pT25ARF6] (Fig. 2 *B* and *C*, 9). Any potential mutation identified in pCTA1$_{R7K}$T18–2 could therefore be separated from the mutation that determines the R7K substitution by recloning the *Xba*I-*Cla*I fragment from the mutant of interest into pCTA1T18–2 or into pARCT4 to construct and characterize variant CT holotoxins containing only the substitutions of interest.

A PCR-generated library of CTA1 variants was constructed in pCTA1$_{R7K}$T18–2, as described in *Materials and Methods*, and transformed into TE1DC[pCT25ARF6]. In the presence of 12.5 μM IPTG, TE1DC strains producing functional CTA1T18 and T25ARF6 fusion proteins were unable to form colonies on maltose–MacConkey media (data not shown). Therefore, clones producing variant CTA1T18 fusion proteins that have lost or decreased their ability to interact with T25ARF6 can be selected by plating on IPTG-containing plates. We found that all colorless transformants failed to produce full-length CTA1T18 fusion proteins, whereas the transformants that produced red colonies made full-length CTA1T18 fusion proteins that presumably had significantly decreased ability to interact with T25ARF6 (data not shown). The latter class of transformants formed colorless or pale pink colonies on media without IPTG (Fig. 2*D*, 10–13), in contrast to strains containing the unmutagenized parental plasmids that formed red colonies on media without IPTG (Fig. 2*D*, 9).

We determined the DNA sequence of the *ctxA1* alleles from selected variants. Where more than one amino acid substitution was found, it was often possible to separate these mutations by subcloning appropriate restriction fragments back into the parental construct. Although all variants produced CTA1T18 fusion proteins that were stable in the cytoplasm of *E. coli*, many of the mutations in the CTA1 coding region prevented formation of holotoxin when they were introduced into a native CT operon (data not shown). Only the variants that formed holotoxin, indicating that their CTA subunits were probably similar in conformation to native CTA, were analyzed further (Table 1; Fig. 2*D*). Quantitative data on the interaction of CTA1 with ARF6 were obtained by transforming the CTA1$_{R7K}$T18–2 variants into DH1DC[pT25ARF6] and by measuring β-galactosidase levels of overnight cultures. The amounts of holotoxin produced by strains with these mutations in the *ctx* operon were also determined and compared for toxicity in the Y1 cell-rounding assay to wt holotoxin also produced in *E. coli*. Additionally, two substitutions (V97K and Y104K) that were previously identified as putative determinants for LT–ARF interaction (27) were constructed by site-directed mutagenesis and also characterized in this system.

The substitutions that affected CTA1–ARF interaction but still allowed CTA to assemble into holotoxin (Table 1) clustered in three regions of CTA1—the α-helical portion of the loop that occludes the active site in the crystal structure of CT (residues between 40–44), an α-helix and β-sheet region that precedes the catalytic residue E112 (residues between 97–104), and the N-terminal portion of the globular A1$_3$ subdomain (residues 167 and 171). The locations of these residues in the CTA1 domain of

Table 1. Characterization of variants of CTA1 showing reduced ARF interaction

Amino acid substitution	β-Galactosidase activity, Miller units*	Variant CT holotoxins†		
		Percent assembly	Trypsin sensitivity	Relative toxicity
Parental (R7K)†	728 ± 43	100	R‡	1
I16A (alone, LC)§	569 ± 43	nd	nd	nd
I16A (alone, HC)	103 ± 8	nd	nd	nd
N40D	222 ± 58	100	R	0.18
L41F	0 ± 1	100	R	<0.003
Y42C	28 ± 1	nd	nd	nd
Y42C+T75A	78 ± 18	100	R	<0.03
T75A	604 ± 228	nd	nd	nd
H44Y	8 ± 1	60	S	<0.004
V97K	13 ± 6	100	R	<0.004
D99N	643 ± 92	100	R	1
Y104K	12 ± 1	50	S	<0.03
F167L	0 ± 0	100	R±	<0.006
R54G	662 ± 207	nd	nd	nd
R54G+H171Y	18 ± 4	nd	nd	nd
H171Y	27 ± 18	100	R	<0.0014

nd, not done.
*Assayed in *E. coli* DH1DC[pCTA1$_{R7K}$T18-2 (or variant), pT25ARF6].
†The CTA1-R7K substitution is not present in the CT holotoxin variants.
‡R, resistant; R±, partially resistant; S, sensitive.
§HC, high copy number vector, LC, low copy number vector, R7K mutation is not present.

MICROBIOLOGY

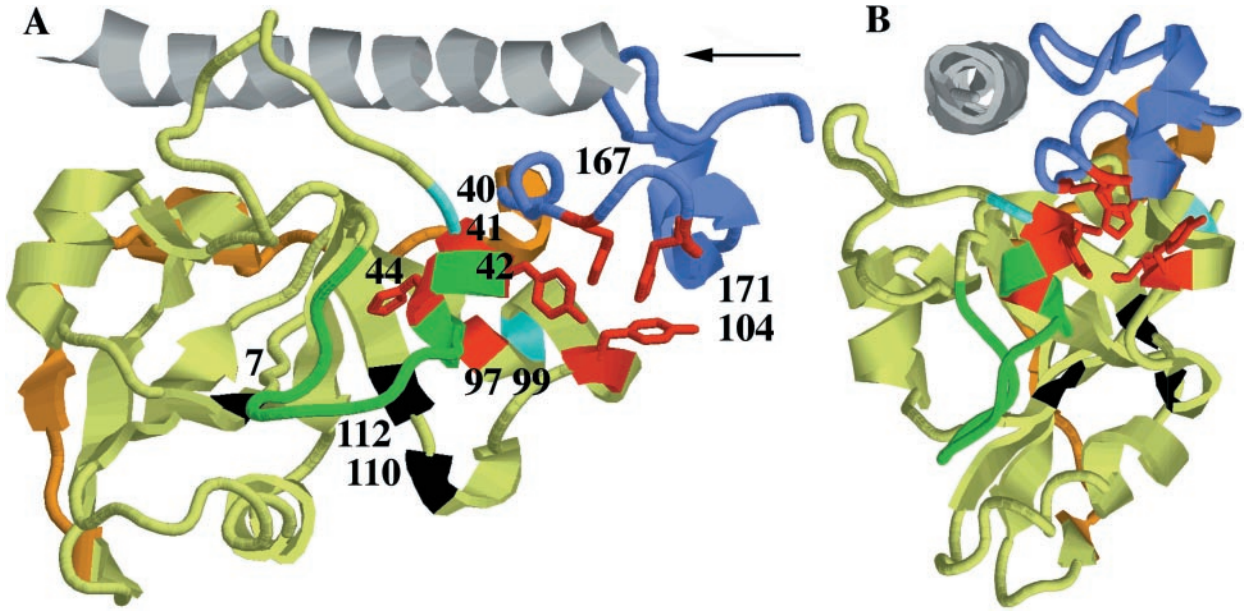

Fig. 3. Cartoon diagram of CTA1 and CTA2 showing residues proposed to interact with ARF6. Only residues 196–226 of CTA2 are shown, in gray. Subdomains of CTA1 are colored light green (globular $A1_1$, 1–132), orange (extended bridge $A1_2$, 133–161), and blue (globular hydrophobic $A1_3$, 162–192). The loop (41–56) that partially occludes the active site is shown in green. Individual residues that affected interaction of CTA1 with ARF6 are colored red, and among these the side chains of the aromatic residues are shown in stick format. Residues 40 and 99 that have only partial effects on ARF interaction are colored cyan. Residues where enzyme-inactivating substitutions (R7K, E110D + E112D) were made in parental constructs are shown in black. (*A*) Individual residues are identified by number. The arrow denotes the point of view for (*B*), down the axis of the A2 α helix.

native CT holotoxin are shown in Fig. 3*A*. These three regions are spatially close to each other and form a relatively compact site in the tertiary structure (Fig. 3*B*). Decreased activity of the CTA1 variants in the two-hybrid system as assessed by β-galactosidase activity correlated well with decreased enterotoxicity of the corresponding variant holotoxins. Substitutions that abolished detectable CTA1–ARF interaction in the two-hybrid system often reduced enterotoxicity several hundred-fold. In contrast, CTA1 substitutions that caused moderate or slightly decreased activity in the two-hybrid system (N40D and D99N) showed slight or no reduction in toxicity of the corresponding variant holotoxins. Furthermore, most of the substitutions did not substantially increase the susceptibility of the variant holotoxins to trypsin, and their A1 subunits in holotoxin were as stable as that of wt CT (data not shown). Exceptions were the variant holotoxins with H44Y or Y104K substitutions, which were degraded completely, and the F167L variant, which showed partial degradation after prolonged incubation with trypsin. Therefore, most of the substitutions identified in this study have specific effects that decrease the interaction of CTA1 with ARF6 and no global effects on the overall conformation of the CTA1 domain.

Discussion

The genetic system reported here is, to our knowledge, the first to demonstrate and quantitate direct interaction between CTA1 and ARF in the bacterial cytoplasm. Using the IPTG-induced lethality of the reporter system, we were able to select variants of CTA1 that exhibited decreased interaction with ARF. It is possible, but unlikely, that these substitutions in CTA1 could affect the ability of the T18 domain in the fusion proteins to interact with the T25 domain in the T25ARF6 fusion protein, thereby reducing the signal. Direct biochemical analysis will be required to confirm the specificity of the interaction between the variants and ARF6. By concentrating on substitutions that permit CTA to assemble into holotoxin that exhibited apparently native conformation, as assayed by susceptibility to proteolysis by trypsin, we were able to define a specific motif in the CTA1 subunit that appears to form the ARF interaction domain. This system should also facilitate future study of the motif in ARF that interacts with CTA1.

It is remarkable that this bacterial system can be used to detect physical binding interaction between CTA1 and ARF. To be functional, ARFs must be in a GTP-bound state, and GTP binding depends highly on the presence of a hydrophobic environment such as a lipid membrane. The N-terminal α-helix of ARF acts as an inhibitory domain that limits GTP binding and confers dependence on lipids (28). In eukaryotic cells, ARFs are also N myristylated, which is critical for correctly associating ARF-GTP with membranes (29). Thus both the N terminus and myristate are critical for normal ARF activities in eukaryotic cells, where they participate in regulating the switch between the inactive cytosolic ARF-GDP and the active membrane-associated ARF-GTP forms (30, 31). The two-hybrid system reported here uses human ARF6 protein. Of all the ARF family members, ARF6 shows the least dependence on lipids for CTA1 activation (30), and it has a shorter N-terminal domain (31). Recombinant ARF6 produced in *E. coli* is not myristylated, but it is capable of activating CTA1 *in vitro* (30). We speculate that positioning the T25 domain at the N terminus of ARF6 in T25ARF6 may prevent the N-terminal α helix of ARF6 from binding in its hydrophobic pocket, thus promoting formation of ARF6-GTP (31). Recently published data also demonstrated *in vitro* that the A1 subunit of *E. coli* heat-labile enterotoxin (LTA1) stimulated ARF3 to adopt fully the GTP-bound conformation (1 mol GTP bound/mol of ARF3 with LTA1 vs. 0.05 mol/mol without LTA1; ref. 32). Further studies are needed to demonstrate whether any or all of these factors facilitate binding between CTA1 and ARF6 in the two-hybrid system described here.

Modulation of the copy number of the compatible plasmid vectors was critical for optimizing the sensitivity of the system. Decreasing the copy number of the plasmid producing the $CTA1_{I16A}T18$ variant (which has reduced enzymatic activity;

unpublished results) increased the signal by 550% with respect to the signal elicited by the same variant expressed from the higher copy number vector (Table 1). Similarly, an enzymatically inactive variant of CTA1 appeared necessary for maximal activity, possibly by decreasing potential toxic effects in *E. coli* of ARF-mediated stimulation of CTA1 enzymatic activity. An alternative explanation could be that the enzymatically inactive variants of CTA1 used in this study (R7K, I16A, or E110D + E112D) caused the CTA1 hybrid protein variants to adopt conformations that are better able to interact with the T25ARF6 hybrid protein. It is known that the homologous R7K substitution in LT holotoxin perturbs its structure (33) and increases the flexibility of residues 47–56 in loop 41–56 that occludes the active site. Interestingly, the N-terminal α-helical portion of the corresponding loop in CT (40–44) appears to participate in binding interactions with ARF. We have structural and immunological evidence for changes in the R7K CT holotoxin variant similar to those reported for the R7K variant of LT (unpublished data), but we did not observe such changes in the I16A or E110D + E112D variant CT holotoxins. These findings suggest it is the decreased enzymatic activity of the CTA1T18 hybrid proteins *per se* rather than substitution-induced conformational changes that produces optimal activity of the two-hybrid assay system.

The three-dimensional structures of CT (34), LT (35, 36), nicked LT (37), and LT-R7K (33) holotoxins are all of the latent enzyme, but structures of the enzymatically active reduced A1 polypeptides of CT or LT are not yet available. Nicking leads to very little if any change in the structure of the A1 subunit in holotoxin, and activation requires reduction of the disulfide bond between Cys-187 and Cys-199 (3). A model for the conformational changes in the A1 subunit during activation of the enzymatic activity of LT and CT has been reported (33). For either enterotoxin, nicking and reduction presumably allow the A1 polypeptide to dissociate from the A2 polypeptide and B pentamer and either expose the ARF interaction interface or change the conformation of the A1 polypeptide to form the ARF interaction interface. Our data are consistent with a conformational change of CTA1 as the explanation for formation of the ARF interaction interface, because the critical residues of CTA1 identified here (residues 41, 42, 104, 167, and 171) are neither involved in interaction with A2 nor buried by the A1-A2 interface. H171, Y104, and Y42, however, are only partially surface exposed. Other residues important for interaction with ARF are buried in the three-dimensional structure of the latent A1 subunit (L41, H44, and F167), possibly requiring they be exposed to interact with ARF. V97 may not interact directly with ARF. Instead, the V97K variant may stabilize the A1 polypeptide in the latent conformation, because it was found to inactivate the enzyme by forming a salt bridge with the catalytic residue E112 in the latent enzyme structure (38).

On the basis of these considerations, we propose the following working model for activation of CTA1 by ARF. First, reduction of the disulfide bond and dissociation of CTA1 from CTA2 permit movement of the A2-interacting loops of the hydrophobic $A1_3$ subdomain, as initially proposed for the first step in activating the ADP-ribosyltransferase function of the A1 fragment (33). The resulting increase in exposure of the aromatic residues F167, H171, Y42, and Y104 may create an initial ARF interaction motif. Additional interaction of ARF with residues between 40 and 44 could promote displacement of the occluding loop (residues 41–56) from the active site, permitting or stimulating NAD binding. Finally, ARF interaction with the α-helix-4 (residues 96–102, V97, and D99) and β-sheet-6 [residues 103–106, Y104, according to Zhang *et al.* (34)] may alter the exact orientation of the active site residues E112 (and E110) to decrease the K_m and increase the V_{max} of the active enzyme. Further testing of this model should provide additional insights into the structural basis for stimulation of the enzymatic activity of the A1 fragments of CT and LT by ARF.

We are grateful for the excellent technical assistance of Brenda Kostelecky. This work was supported in part by Grant AI31940 (to R.K.H.) from the National Institutes of Health.

1. Kaper, J. B., Morris, J. G., Jr. & Levine, M. M. (1995) *Clin. Microbiol. Rev.* **8,** 48–86.
2. Spangler, B. D. (1992) *Microbiol. Rev.* **56,** 622–647.
3. Mekalanos, J. J., Collier, R. J. & Romig, W. R. (1979) *J. Biol. Chem.* **254,** 5855–5861.
4. Galloway, T. S. & van Heyningen, S. (1987) *Biochem. J.* **244,** 225–230.
5. Moss, J. & Vaughan, M. (1993) *Cell. Signalling* **5,** 367–379.
6. Lee, C. M., Chang, P. P., Tsai, S.-C., Adamik, R., Price, S. R., Kunz, B. C., Moss, J., Twiddy, E. M. & Holmes, R. K. (1991) *J. Clin. Invest.* **87,** 1780–1786.
7. Moss, J. & Vaughan, M. (1998) *J. Biol. Chem.* **273,** 21431–21434.
8. Roth, M. G. (1999) *Cell* **97,** 149–152.
9. Al-Awar, O., Radhakrishna, H., Powell, N. N. & Donaldson, J. G. (2000) *Mol. Cell. Biol.* **20,** 5998–6007.
10. Altschuler, Y., Liu, S., Katz, L., Tang, K., Hardy, S., Brodsky, F., Apodaca, G. & Mostov, K. (1999) *J. Cell. Biol.* **147,** 7–12.
11. Boshans, R. L., Szanto, S., van, A. L. & D'Souza-Schorey, C. (2000) *Mol. Cell. Biol.* **20,** 3685–3694.
12. Moss, J. & Vaughan, M. (1999) *Mol. Cell. Biochem.* **193,** 153–157.
13. Noda, M., Tsai, S.-C., Adamik, R., Moss, J. & Vaughan, M. (1990) *Biochim. Biophys. Acta* **1034,** 195–199.
14. Moss, J., Stanley, S. J., Vaughan, M. & Tsuji, T. (1993) *J. Biol. Chem.* **268,** 6383–6387.
15. Karimova, G., Pidoux, J., Ullmann, A. & Ladant, D. (1998) *Proc. Natl. Acad. Sci. USA* **95,** 5752–5756.
16. Jobling, M. G., Palmer, L. M., Erbe, J. L. & Holmes, R. K. (1997) *Plasmid* **38,** 158–173.
17. Shah, S. & Peterkofsky, A. (1991) *J. Bacteriol.* **173,** 3238–3242.
18. Hanahan, D. (1983) *J. Mol. Biol.* **166,** 557–580.
19. Sektas, M., Gregorowicz, M. & Szybalski, W. (1999) *BioTechniques* **27,** 911–914.
20. Chang, A. C. & Cohen, S. N. (1978) *J. Bacteriol.* **134,** 1141–1156.
21. Tabor, S. & Richardson, C. C. (1985) *Proc. Natl. Acad. Sci. USA* **82,** 1074–1078.
22. Miller, J. H. (ed.). (1972) *Experiments in Molecular Genetics* (Cold Spring Harbor Lab. Press, Plainview, NY).
23. Pérez-Pérez, J. & Gutiérrez, J. (1995) *Gene* **158,** 141–142.
24. Holmes, R. K. & Twiddy, E. M. (1983) *Infect. Immun.* **42,** 914–923.
25. Maneval, D. R., Colwell, R. R., Grays, S. W. J. & Donta, S. T. (1981) *J. Tissue Cult. Methods* **6,** 85–90.
26. Ladant, D., Michelson, S., Sarfati, R., Gilles, A. M., Predeleanu, R. & Barzu, O. (1989) *J. Biol. Chem.* **264,** 4015–4020.
27. Stevens, L. A., Moss, J., Vaughan, M., Pizza, M. & Rappuoli, R. (1999) *Infect. Immun.* **67,** 259–265.
28. Kahn, R. A., Randozzo, P., Serafini, T., Weiss, O., Rulka, C., Clark, J., Amherdt, M., Roller, P., Orci, L. & Rothman, J. E. (1992) *J. Biol. Chem.* **267,** 13039–13046.
29. Goldberg, J. (1998) *Cell* **95,** 237–248.
30. Price, S. R., Welsh, C. F., Haun, R. S., Stanley, S. J., Moss, J. & Vaughan, M. (1992) *J. Biol. Chem.* **267,** 17766–17772.
31. Menetrey, J., Macia, E., Pasqualato, S., Franco, M. & Cherfils, J. (2000) *Nat. Struct. Biol.* **7,** 466–469.
32. Zhu, X., Boman, A. L., Kuai, J., Cieplak, W. & Kahn, R. A. (2000) *J. Biol. Chem.* **275,** 13465–13475.
33. van den Akker, F., Merritt, E. A., Pizza, M. G., Domenighini, M., Rappuoli, R. & Hol, W. G. J. (1995) *Biochemistry* **34,** 10996–11004.
34. Zhang, R. G., Scott, D. L., Westbrook, M. L., Nance, S., Spangler, B. D., Shipley, G. G. & Westbrook, E. M. (1995) *J. Mol. Biol.* **251,** 563–573.
35. Sixma, T. K., Pronk, S. E., Kalk, K. H., Wartna, E. S., van Zanten, B. A., Witholt, B. & Hol, W. G. (1991) *Nature (London)* **351,** 371–377.
36. Sixma, T. K., Kalk, K. H., van Zanten, B. A. M., Dauter, Z., Kingma, J., Witholt, B. & Hol, W. G. (1993) *J. Mol. Biol.* **230,** 890–918.
37. Merritt, E. A., Pronk, S. E., Sixma, T. K., Kalk, K. H., van Zanten, B. A. M. & Hol, W. G. J. (1994) *FEBS Lett.* **337,** 88–92.
38. Merritt, E. A., Sarfaty, S., Pizza, M., Domenighini, M., Rappuoli, R. & Hol, W. G. (1995) *Nat. Struct. Biol.* **2,** 269–272.